2006 CEDAR Workshop
Eldorado Hotel
Santa Fe, New Mexico, USA
June 19 - 23, 2006

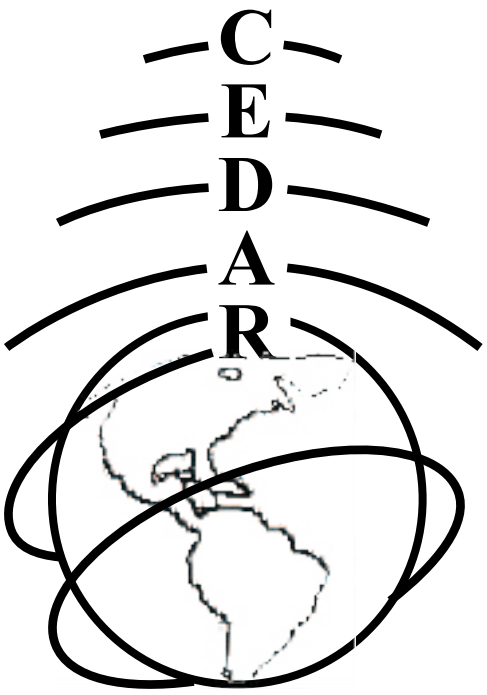

Thursday CEDAR Poster Session Booklet
June 22

Table of Contents

I. Instruments or Techniques for Middle Atmospheric Observation

II. Coupling of the Upper Atmosphere with Lower Altitudes

III. Mesosphere or Lower Thermosphere General Studies

IV. Mesosphere and Lower Thermosphere Gravity Waves

V. Mesosphere and Lower Thermosphere Other Tidal or Planetary Waves

VI. Meteor Science other than Wind Observations

VII. Sprites

VIII. Extraterrestrial Planetary Atmospheres

Instruments or Instruments or Techniques for Middle Atmospheric Observation

ITMA-01 On middle-atmospheric Doppler-Cabanne lidar wind measurements - by Zhaoai Yan

Status of First Author: Student NOT in poster competition, Masters

Authors: Zhao-ai Yan(1)(2) , Jia Yue(2) , David Kruger(2), Chiao-Yao She(2), Johnathan W.Hair(3), Jin-Jia Guo(1), Song-Hua Wu(1), Zhi-Shen Liu(1)
(1)Ocean Remote Sensing Institute, Ocean University of China, Qingdao 266003, China
Email:yanza@orsi.ouc.edu.cn
(2)Physics Department, Colorado State University, Fort Collins, CO. 80523, U. S. A.,
Email: jyue@lamar.colostate.edu
(3)NASA/Langley Research Center, Hampton, Virginia 23681, U. S. A., Email: j.w.hair@larc.nasa.gov

Abstract: Two techniques for frequency analysis are currently employed by different research groups utilizing direct-detection methods for middle-atmospheric lidar wind measurements, the double-edge Fabry-Perot interferometer (FPI) and the iodine vapor filter(IVF). The performances of double-edge FPI at 355nm (uv-FPI) and double-edge IVF at 532nm (de-IVF) with nearly the same maximum transmission of ~80%, are compared and discussed for potential middle-atmospheric applications. We found that the wind uncertainty at the low-wind speed is lowest with uv-FPI under aerosol free conditions, while the de-IVF yields better performance when aerosol backscatter mixing ratio exceeds 0.015. Though the measurement error using de-IVF is ~30% higher, its simplicity and relatively low-cost implementation merits consideration for stratospheric and mesospheric applications. Projected measurement accuracies as a function of power-aperture product and altitude will be discussed.

ITMA-02 Planar Array Design in Meteor Radar Systems - by Chunmei Kang

Status of First Author: Student IN poster competition, PhD

Authors: Chunmei Kang and Scott E. Palo
Department of Aerospace Engineering Sciences
University of Colorado, Boulder, CO, 80309

Abstract: Interferometric techniques are commonly used in all-sky meteor radar systems for meteor location determination. Essentially, interferometric techniques use the phase information recorded from different receiving antennas to estimate the elevation and azimuth of meteors. Prior efforts have been made to determine an antenna geometry that improves the performance of meteor radar systems. For example, Hocking and Thayaparan (1997) used four antennas typically spaced by 1.5 to 3 wavelengths to locate the meteors. Jones (1992) and Hocking (1997) presented an antenna geometry using a 5 element array with minimum antenna spacing of 2 wavelengths to estimate the direction of arrival (DOA) of the meteors. By spacing the antennas more than 2 wavelength apart, these array geometries were successful in reducing the electromagnetic coupling effect between the antennas, which can introduce errors in the estimation of meteor locations. However, even though the condition of 2 wavelength spacing is satisfied, a limited number of sensors as well as their positioning will create deficient spatial sampling of the incident signal and can induce biases in DOA estimates.

In this work, we evaluate potential array geometries by computing their accuracy and precision. The metrics that we use are the Cramer-Rao bound (CRB), the co-array and the beam pattern. Four array geometries are examined herein, which include the cross, T, L, and circular arrays and all are implemented with 5 elements. We demonstrate that for the CObRa meteor radar system, using a coarse search with the yagi antennas, the circular array performs better in reducing biases than all the other geometries and has a CRB level comparable to the cross array. For a general all-sky meteor radar system, the T array performs best with an overall resolution and CRB than exceeds the other geometries. The cross array, currently used by most all-sky meteor radar systems is shown to exhibit the worst performance of the group.

To evaluate the accuracy impact of the specified array geometries a maximum likelihood (ML) DOA estimator was constructed. Estimates using a range of signal to noise ratios are evaluated to determine the potential biases of each array geometry, Additionally a MATLAB-based planar array design assistant package is discussed. This software package was implemented primarily to visualize the direction of arrival (DOA) estimator performance for an arbitrary user specified array. Performance comparisons of nominal array geometries are also provided.

ITMA-03 An all-solid-state transportable narrowband sodium lidar for mesopause region temperature and horizontal wind measurements - by Jia Yue

Status of First Author: Student IN poster competition, PhD

Authors: Jia Yue, Phil Acott, Joe Vance, Joe She,
Colorado State University, Fort Collins, CO jyue@lamar.colostate.edu
Qian Wu, NCAR, Boulder, CO
Bifford Williams, CORA, Boulder, CO
Richard Collins, U of Alaska, Fairbanks, AK

Abstract: We describe a proposed all solid-state narrowband sodium lidar. The new lidar will implement the Colorado State University (CSU) Doppler-free spectroscopic seed control and resultant highly accurate laser locking with a low-power continuous-wave sum-frequency generator (SFG) into the Shinshu University solid-state sodium temperature lidar system. Together with the sodium-vapor Faraday filters in the receiver, the proposed lidar system is capable of measuring both mesopause-region temperature and horizontal wind on 24-hour continuous basis, weather permitting. The all solid-state lidar will be housed into a trailer with necessary electronics and data acquisition devices, which is suitable for mobile deployment and remote operation. The advantages of CSU Doppler-free spectroscopy, low-power SFG and Faraday filter have been proven in CSU lidar and Weber lidar system over many years. This paper emphasizes a new low-power SFG is under construction and testing at CSU. The deployment of this mobile lidar in concert with radars like AMISR and other passive instruments will provide, otherwise lacking, high resolution comprehensive measurements of atmospheric states and waves in the mesopause region.

ITMA-04 The Study of Beam Broadening Effect on Doppler Spectrum - by Meng-Yuan Chen

Status of First Author: Student NOT in poster competition, PhD

Authors: Meng-Yuan Chen and Yen-Hsyang Chu
Institute of Space Science, National Central University, Chung-Li, Taiwan.

Abstract: The observed Doppler spectrum can be affected by several effects including the beam width, wind shear, wind velocity and direction. The numerical simulation of Doppler spectral width due to beam broadening t and wind shear effects, which are not entirely independent, is presented in this study. The analytic solution of a simple 2-dimensional non-shear model is also derived. Comparisons show that the 2-dimensional model underestimates the beam broadening spectral width. Moreover, it has been shown that the beam broadening spectral width for an oblique beam is not only determined by antenna beam width and wind shear but also a function of wind velocity and direction in this article. Each effect should be taken into account in estimating atmospheric parameters from the observed spectral width with Doppler radars.

ITMA-05 The Sodium Faraday Filter and Daytime Lidar Observations: A History and Current Developments - by Sean Harrell

Status of First Author: Student IN poster competition, PhD

Authors: Sean Harrell Colorado State University, Tao Yuan CSU, Biff Williams now with NorthWest Research Associates CoRA Division, David A. Krueger CSU, and Joe She CSU

Abstract: The sodium vapor Faraday filter developed at Colorado State University uses a sodium vapor cell in an axial magnetic field between crossed polarizers to filter out light that is not within ~ 10 GHz of the sodium resonance transition at 589 nm. This allows continuous, day and night use of the CSU sodium lidar to make measurements of mesopause region temperature and horizontal winds. The history, current status and a novel potential improvement of the Faraday filters will be reviewed. The emphasis of this paper will be on a modification of cell tip-off arrangement and temperature control under construction, which promises to increase the robustness of the Faraday filter for long-period campaigns and remote operation.

ITMA-06 High-resolution remote sensing of mesospheric carbon monoxide - by Chris Martin

Status of First Author: Non-student

Authors: C. L. Martin and S. M. Burrows

Abstract: We present high-resolution ground-based measurements of mesospheric CO from the AST/RO sub-millimeter telescope, located at the Amundsen-Scott South Pole Station. These include the first winter measurements of CO directly from

one of the geographic poles, providing confirming evidence for predicted high concentrations within the polar vortex. We also use CO as a tracer to estimate mesospheric neutral wind speeds, using small Doppler shifts in the rotational spectrum. We argue that high-resolution measurements of CO rotational spectra could provide a new method for direct measurement of mesospheric winds, filling a significant experimental data gap.

ITMA-07 Tomographic Estimations of Vertical Airglow Profiles - by D. Scott Anderson

Status of First Author: Student NOT in poster competition, PhD

Authors: Gary Swenson, University of Illinois
Farzad Kamalabadi, University of Illinois

Abstract: The observation of airglow emissions from the ground using CCD imagers can be represented as the projection of the three-dimensional airglow structure onto an image. As such, the use of multiple imagers on the ground presents the opportunity to formulate the reconstruction of the airglow as a linear, weighted least-squares optimization. Unfortunately, since the projections of the airglow are over a limited angle (from the ground) and due to the geometry of the problem, there are strict limitations to which spatial frequencies of the structure can be reconstructed. This limitation, which can be understood through the Fourier Slice Theorem, governs the likelihood of recovering the perturbation structure and vertical profile of the airglow. In this work, we present an airglow model with characteristic atmospheric-gravity-wave-induced perturbations and a vertical profile. We describe the problem's forward projection representation and its solution as a weighted least-squares optimization with a priori regularization. We then demonstrate the successful reconstruction of the perturbation structure in the airglows as well as the inherent inability to directly reconstruct the vertical profile due to the lack of Fourier support provided by the projection data. Finally, we present the intended future direction of this research, which, immediately, is to apply the reconstruction scheme to the airglow imagery taken during the ALOHA 93 campaign.

ITMA-08 Ground-based mesospheric OH temperature comparisons with simultaneous TIMED SABER temperatures over Millstone Hill - by Steven M Smith

Status of First Author: Non-student

Authors: S.M. Smith1,
J. Baumgardner1,,C.J. Mertens2, J.M. Russell3, M.G. Mlynczak2, M. Mendillo1
1Center for Space Physics, Boston University, Boston, MA 02215
2NASA Langley Research Center, Hampton, VA 23681
3Center for Atmospheric Sciences, Hampton University, Hampton, VA 23668

Abstract: We present a cross-validation study of ground-based rotational temperature measurements from the mesospheric OH emission layer at Millstone Hill (42.6ºN, 72.5ºW) with near-simultaneous space-based kinetic temperature measurements from the TIMED SABER instrument during overpasses of Millstone Hill. The measurements were made on fourteen nights during August and September 2005. Although only a small preliminary dataset was used, excellent agreement was obtained between the two datasets, and the comparison appeared to validate the both sets of measurements and the methods used to derive them. The small differences can be attributed to differences in the spatial and temporal averaging inherent in two datasets. The new ground-based spectrographic measurements will greatly enhance the mesospheric work done already at Millstone Hill. The ongoing SABER measurements will complement this effort by providing OH emission layer height and shape and temperature profile information.

ITMA-09 On the variability of mesospheric OH layer volume emission profiles derived from SABER limb measurements - by Romina Nikoukar

Status of First Author: Student NOT in poster competition, PhD

Authors: R. Nikoukar - UIUC - nikoukar@uiuc.edu
F. Kamalabadi - UIUC - farzadk@uiuc.edu
G. Swenson - UIUC - swenson1@uiuc.edu
A. Liu - UIUC - liuzr@ad.uiuc.edu

Abstract: Mesospheric OH radiance limb profiles measured by SABER instrument aboard the TIMED spacecraft were inverted to yield altitude profiles of OH volume emission rates (VER). The inversion was performed using the Abel transform and a tomographic technique, with nearly identical results. The inversion results were analyzed for the layer variance as a function of

latitude, local time and season. The results of this analysis show that the profiles exhibit larger variance at heights lower than the mean peak, over an altitude range with less thickness than the mean layer, similar to the model predictions by Liu and Swenson (2003). These variations from the mean are likely caused primarily by diurnal tides and atmospheric waves, and hence their characterization can be used to derive wave parameters.

ITMA-10 A new receiving system for SuperDARN meteor echo detection and analysis - by Richard Todd Parris

Status of First Author: Student IN poster competition, PhD

Authors: William A. Bristow, Geophysical Institute, University of Alaska Fairbanks

Abstract: The SuperDARN HF radar on Kodiak Island, Alaska, has been upgraded with a new receiving system that greatly improves the range resolution of meteor echo detections. The new resolution afforded by this upgrade greatly increases the utility of the radar as a tool for studying dynamics in the MLT region. The details of the receiver upgrade, a discussion of the radar analysis techniques used detect meteor echoes and extract useful information from the detections will be presented. An example of meteor region wind analysis, which is now possible with the new recieveing system, will also be presented.

ITMA-11 Magnetic Fields Measurments of the Mesosphere Using the Zeeman Splittling of O-18O - by Michael John Brown

Status of First Author: Student NOT in poster competition, Undergraduate

Authors: Michael Brown (mjbrown@oberlin.edu)
Chris Martin (cmartin@oberlin.edu)

Abstract: Microwave Spectra were taken from Antarctica during January of 2005. The Zeeman splitting observed in the spectra were then used to calculate the magnetic field in the mesosphere. These calculated values were then correlated with the magnetic field on the ground from a land based magnetometer.

Coupling of the Upper Atmosphere with Lower Altitudes

COUP-01 Relation of the plasmapause to the outer radiation belt from DMSP, IMAGE, and SAMPEX observations - by William Robert Johnston

Status of First Author: Student IN poster competition, PhD

Authors: Wm. Robert Johnston, Phillip C. Anderson, Jerry Goldstein, and Shrikanth G. Kanekal

Abstract: The plasmapause separates cold dense plasma in the inner magnetosphere from hot, low density plasmasheet ions. This boundary, typically at 4-6 Re, tends to show a duskside bulge but is also very dynamic in response to changes in magnetospheric convection and other stormtime phenomena. The outer radiation belt is likewise dynamic during stormtime, in terms of both radial location and energetic particle population. It has been

proposed that outer radiation belt particles are variously depleted and energized due to wave-particle interactions associated with the plasmapause location. This may be tested by simultaneous observations of energetic particles and the plasmapause location. SAMPEX observations of radiation belt particles may be compared with plasmapause observations from IMAGE, but these provide limited temporal coverage. We will use data from DMSP satellites to identify the plasmapause signature in the ionosphere (specifically the light ion trough) to provide more continuous plasmapause observations. Initial comparisons of DMSP-derived plasmapause locations to IMAGE-based observations as well as outer radiation belt dynamics from SAMPEX show good correlations.

COUP-02 The Aeronomy of Auroral Ion Upflow - by Matthew D Zettergren

Status of First Author: Student IN poster competition, Masters

Authors: Matthew Zettergren, Joshua Semeter, Kristina Lynch, Pierre-Louis Blelly

Abstract: In this research we simulate the effects of the electron precipitation measured by the SIERRA rocket experiment on the ionosphere. The SIERRA experiment measured a soft downward flux of superthermal electrons concurrent with a upward flow of oxygen ions. This soft flux is not energetic enough to cause a significant

ionization increase. However, our simulations show that the precipitating electrons heat the ambient electrons in the ionosphere and cause atomic excitation and optical emission. The heating causes an electron pressure increase, which, in turn, sets up an ambipolar electric field that accelerates the ions upward along the magnetic field line. A large upward flux of oxygen ions is predicted by our simulation in response to the soft flux. Ion velocities exceed 2 km/s, which is consistent with radar measurements that have been made during previous soft flux events. The ambipolar electric field has been implicated before in causing large oxygen ion upflows, but evidence for other mechanisms such as ion-acoustic turbulence have also been suggested. Our work will look to resolve the exact cause of large-scale ion upflow in the ionosphere. Various optical emission wavelengths predicted by our model are also examined in order to classify this type of event by based on the type of optical emission spectrum that it produces.

COUP-03 Gravity Waves in the Lower Stratosphere at South Pole - by Zhenhua Li

Status of First Author: Non-student PhD

Authors: Li, Zhenhua (zli2@uiuc.edu),
Robinson, Walter, Department of Atmospheric Sciences, University of Illinois at Urbana-Champaign
Liu, Alan Z., Department of Electrical and Computer Engineering, University of Illinois at Urbana-Champaign

Abstract: We characterize gravity waves in the lower stratosphere at South Pole using high-resolution balloon soundings from 1993 to 2005. South Pole is an interesting site for gravity-wave studies because it is remote from most likely sources of gravity waves: topographic relief and regions of convective and synoptic activity. A comprehensive analysis is performed for the gravity-wave energy density, vertical wavenumber spectra, and stability. The relationships between the background structures of temperature and wind and the strength of gravity wave activity at South Pole are examined. Gravity wave perturbations in the lower stratosphere are strongest during austral spring and fall when cooling/warming descends from the upper-stratosphere and climatological winds are strong. We also investigate relationships between the gravity waves and the tropospheric synoptic-scale variations over and around Antarctica. Enhanced gravity-wave activity over South Pole occurs in months with enhanced synoptic activity at certain locations along the Antarctic coast. We interpret these relationships as resulting from a convolution of the influences of synoptic activity, strong topographic relief, and mean winds that favor the propagation of the gravity waves from the some regions of the coast to the lower stratosphere above South Pole.

COUP-04 Broadband VLF measurement of D region ionospheric perturbations caused by lightning electromagnetic pulses - by Zhengang Cheng

Status of First Author: Student IN poster competition, PhD

Authors: Zhenggang Cheng and Steven A. Cummer
Department of Electrical and Computer Engineering, Duke University, Durham, North Carolina 27708
Han-Tzong Su and Rue-Ron Hsu
Department of Physics and Earth Dynamic System Research Center, National Cheng Kung University, Tainan 70101, Taiwan

Abstract: The first experimental evidence of the impulsive direct coupling of energy released by lightning discharge to the lower ionosphere was reported in the form of early/fast perturbation on sub-ionospherically propagating very low frequency (VLF) signals. Since then, based on modeling and measurements, different mechanisms have been advanced to explain the fast sub-ionospheric VLF perturbations, such as the ionization and heating associated with elves or electrical breakdown associated with sprites and halos. By comparing the broadband VLF spectra (3-25 kHz) of lightning discharges that occurred immediately (<15 s) after intense lightning discharges (>60 kA peak current) with the spectra of lightning discharges that were not preceded by an intense lightning discharge within approximately 60 seconds, we detect D region disturbances caused by these intense lightning flashes over the U.S. East Coast and the U.S. High Plains. The detailed electron density changes caused by the disturbances are measured by analyzing the broadband VLF propagation changes, and the perturbed electron density profiles from both regions are found to be consistent with those theoretically predicted for strong lightning electromagnetic pulses and also not consistent with perturbations produced by other mechanisms. In one special case, a D region perturbation is detected following a lightning stroke that produced an isolated elve according to the records by ISUAL satellite, confirming that we are measuring lightning-EMP associated VLF perturbations. In this case, we find electron density enhancements of ~460 cm-3 averaged over a ~220 km radius and 10 km high perturbation region, within a factor of ~2 of the 210 cm-3 measured by Mende et al. [2005] for a single elve event. The characteristics of the lightning responsible for these perturbations are investigated by comparing high peak current lighting strokes that do and do not generate detectable ionospheric perturbations. Overall, we find that at least some detectable broadband VLF perturbations are created by intense lightning-EMP that produces detectable optical emissions (elves) in the strongest cases.

COUP-05 Electrical structure of thunderclouds leading to formation of blue jets and gigantic jets - by Jérémy Riousset

Status of First Author: Student IN poster competition, Masters

Authors: Jérémy A. Riousset (jar471@psu.edu), Victor P. Pasko (vpasko@psu.edu), Paul R. Krehbiel (krehbiel@ibis.nmt.edu), William Rison (rison@ee.nmt.edu), Ronald J. Thomas (thomas@nmt.edu)

Abstract: Blue jets and gigantic jets are transient luminous events, which develop upwards from thundercloud tops to terminal altitudes ranging from 40 to 90 km [Wescott et al., GRL, 22(10), 1209–1212, 1995; JASTP, 60, 713–724, 1998; Pasko et al., Nature, 416, 152–154, 2002; Lyons et al., BAMS, 84(4), 445–454, 2003; Su et al., Nature, 423, 974–976, 2003]. It is believed that these events represent a stage of development of conventional lightning leaders near thundercloud tops when the combination of electric field distribution created by thundercloud charges and reduction of atmospheric neutral density with altitude create favorable conditions for their upward development [e.g., Pasko and George, JGR, 107(A12), 1458, 2002; Moss et al., JGR, 111, A02307, 2006; Pasko, NATO Sci. Ser. II, 225, 253–311, 2006, and references therein]. It is generally recognized that the direct comparison of lightning mapping observations by the New Mexico Tech Lightning Mapping Array (LMA) with realistic models of thundercloud electrical structure and lightning discharges represents a useful tool for studies of electrification mechanisms in thunderstorms, initiation and propagation mechanisms of different types of lightning discharges as well as for understanding of electrical and energetic effects of tropospheric thunderstorms on the upper regions of the Earth's atmosphere. The goal of this presentation is twofold. First, we will present the formulation of a new three-dimensional probabilistic model describing development of bi-directional structure of positive and negative lightning leaders closely resembling processes observed by LMA in association with intra-cloud discharges. The model represents a synthesis of the original dielectric breakdown model based on fractal approach proposed by Niemeyer et al. [PRL, 52(12), 1033–1036, 1984] and the equipotential lightning channel hypothesis advanced by Kasemir [JGR, 65(7), 1873–1878, 1960], and places special emphasis on obtaining self-consistent solutions preserving complete charge neutrality of the discharge trees at any point during the simulation. We will present comparisons of model results and a representative progression of lightning leaders measured by LMA indicating that the model is capable of realistically reproducing principal features of the observed lightning events. Second, we will present model-based analysis of realistic charge distributions in thunderclouds creating favorable conditions for upward extension of leaders leading to formation of blue jets and gigantic jets. Special emphasis will be placed on discussion and accurate model description of terminal altitudes of blue jets and gigantic jets based on the "moving capacitor plate" model formulated in [Greifinger and Greifinger, JGR, 81(13), 2237–2247, 1976] and further discussed with application to blue jet type of phenomena in [Pasko and George, 2002; Pasko, 2006, and references therein].

COUP-06 Observational Study of the Arctic Middle Atmosphere Using Lidar, Satellite, and meteorological Measurements and Analyses - by Brentha Thurairajah (presented by Richard Collins)

Status of First Author: Student NOT in poster competition, PhD

Authors: Brentha Thurairajah, Ruth S. Lieberman, Dennis M. Riggin, V. Lynn Harvey, Kazuyo Sakanoi, Kohei Mizutani, Richard L. Collins

Abstract: Recent studies indicate that there are connections between the middle atmosphere (stratosphere and mesosphere) circulation and climate oscillations in the troposphere. Changes in the polar vortex and related indices like the Arctic Oscillation, may affect the Arctic climate. To understand the coupling between the lower and middle atmospheres a comprehensive analysis of the circulation of the Arctic atmosphere is essential. A preliminary observational study of the Arctic middle atmosphere during January 2003, which combines Rayleigh lidar measurements from Poker Flat Research Range (PFRR), Chatanika, Alaska (65oN, 147oW), TIMED satellite measurements from the Sounding of the Atmosphere using Broadband Emission Radiometry (SABER) instrument, MSIS data, United Kingdom Meteorological Office (UKMO) synoptic maps, and 3D analysis of the Arctic vortex/Aleutian High anticyclone is presented. This analysis provides a foundation for the proposed observational and modeling study of the Arctic stratosphere and mesosphere Pan-Arctic Study of the Stratospheric and Mesospheric Circulation, (PASSMeC) during the International Polar Year (IPY).

COUP-07 Coupling in the mesosphere and lower thermosphere through tidal features observed in OH (6,2) and O2 Atm (0,1) nightglow emissions - by Charles Mutiso

Status of First Author: Student IN poster competition, Masters

Authors: C. Mutiso, S.M.I Azeem, G.G Sivjee, D. Shen
Embry-Riddle Aeronautical University

Abstract: Tidal features have been detected in simultaneous OH Meinel (6,2) and O2 atmospheric (0,1) rotational temperatures obtained during 2002 and 2003 at Adelaide, Australia (34.9 S, 138.6 E). Rotational temperatures obtained from the OH (6,2) and the O2 atm (0,1) bands are in general agreement and exhibit the same gross trends as kinetic temperatures obtained from SABER, in spite of the inherent differences in the retrieval methods. In particular, the OH (6,2) temperatures and SABER temperatures at ~87 km show excellent agreement. Wavelike modulations and tidal spectral peaks at 6, 8 and 12 hours were simultaneously observed in the rotational temperatures of the OH (6,2) and the O2 atm (0,1) bands. Because the two bands peak at different altitudes (~87 km and 95 km, respectively), the amplitudes and phases at the two altitudes are used to determine vertical wavelengths and phase speeds, and to investigate coupling between the mesosphere and lower thermosphere. In addition, variations in the seasonal and annual amplitudes of the tides are analyzed to investigate non-linear coupling and modulation by planetary waves.

COUP-08 An Analysis of the Momentum Forcing in the High-latitude Lower Thermosphere - by Young-Sil Kwak

Status of First Author: Non-student

Authors: Young-Sil Kwak, High Altitude Observatory, National Center for Atmospheric Research
yskwak@ucar.edu
Arthur D. Richmond,High Altitude Observatory, National Center for Atmospheric Research
richmond@ucar.edu

Abstract: To understand the physical processes that control the high-latitude lower thermospheric dynamics, we quantify the forces that are mainly responsible for maintaining the high-latitude lower thermospheric wind system in the summer southern hemisphere with the aid of the National Center for Atmospheric Research Thermosphere-Ionosphere Electrodynamics General Circulation Model (NCAR TIE-GCM). Forces are statistically analyzed in magnetic coordinates as a function of altitude, and their properties for negative IMF Bz are examined. It is confirmed that the transition of the forcing patterns and their relative contribution to the high-latitude lower thermospheric wind system occurs around 123 km under various conditions – weak or strong IMF, summer or winter. Above 123 km the primary forces that determine the neutral circulation are the Coriolis, horizontal momentum-advection, pressure-gradient and ion-drag (mainly rotational Pedersen ion-drag) forces. The Coriolis, horizontal momentum-advection and pressure-gradient accelerations tend to be approximately curl-free and balanced. The wind has a significant influence on the ion drag. The ion-drag acceleration above 123 km is mainly rotational, and makes the dominant contribution to the time-rate-of-change of the largely rotational wind. Below 123 km the horizontal momentum advection tends to be much weaker, and the main forces are the pressure-gradient and Coriolis forces, although there is a significant contribution by the non-rotational Hall ion-drag force in the polar cap. When the negative IMF Bz intensifies from –2.0 nT to –10.0 nT, at higher altitudes (>=123 km) the stronger anticyclonic dusk vortex is sustained by balancing of the enhanced Coriolis and horizontal momentum advection accelerations, and extends to subauroral latitudes. At lower altitudes (< 123 km), a weak cyclonic vortex, as part of the dawn cell, is mainly determined by the enhanced pressure-gradient and Coriolis forces. The neutral winds and forces in the northern winter high latitudes, at higher altitudes (>=123 km), tend to be much weaker than those in the southern summer hemisphere. A relatively strong anticyclonic dusk cell in the winter hemisphere is maintained by balancing of the Coriolis force and the horizontal momentum advection. At lower altitudes (< 123 km), especially on the morning side, the pressure-gradient and Coriolis forces in the winter hemisphere are stronger than those in the summer hemisphere, and sustain a slightly stronger wind than summer wind.

COUP-09 Ionosphere-Thermosphere Response to the April 2002 Magnetic Storm - by Mariangel Fedrizzi

Status of First Author: Non-student PhD

Authors: M. Fedrizzi, T.J. Fuller-Rowell, M. Codrescu, E.A. Araujo-Pradere, N. Maruyama, D. Anderson, A. Anghel, C.F. Minter, T.W. Garner

Abstract: The April 2002 storm event was not one of the most severe magnetic storms that occurred during the Solar Cycle 23. Nevertheless, large CMEs and one of the largest solar flares of the current solar cycle impacted the Earth's space environment during this storm period. In this study, a global, three-dimensional, time-dependent, non-linear coupled model of the thermosphere, ionosphere, plasmasphere, and electrodynamics (CTIPe) is used to examine and analyse the relative contribution of various physical mechanisms responsible for the ionosphere-thermosphere response to the April 2002 event. Horizontal thermospheric winds, thermal expansion and electric fields are amongst the investigated mechanisms. Comparison of the simulations with a range of space and ground-based data are used to help identify the role of each mechanism in the ionosphere-thermosphere response.

COUP-10 Observation of low latitude red aurora on 29 October, 2003 - by Jong-Kyun Chung

Status of First Author: Non-student

Authors: J.-K. Chung, Q. Wu, and S. Solomon, High Altitude Observatory, NCAR
Y. H. Kim, Dept. of Astronomy & Space Science, Chungnam National University
Y.-I. Won, Dept. of Physical Sciences, Embry-Riddle Aeronautical University
J. U. Park and B. G. Choi, Space Geodesy Research Group, Korea Astronomy & Space Science Institute

Abstract: On 28 October 2003, an extreme solar activity triggered an intense geomagnetic storm (Kp > 7) around the Earth during following days. Enhancement of 630.0 nm emission in arc shape was observed through an all-sky camera at Mt. Bohyun (geomagnetic latitude = 29) in Korea at 17:48-18:40 UT on 29 October, during the main phase of the geomagnetic storm. The maximum brightness of the red arc was about 700 R in the northern sky at Mt. Bohyun. Images with the OI 557.7 nm filter did not show any corresponding feature to the observed red arc, implying its aurora nature rather than lower atmospheric phenomena. The red arc lasted less than an hour and moved southwest before fading out. The observed arc in all-sky images is located on the map in the area between L values of 1.4 and 1.6, by assuming its maximum emission height of 400 km. The electron density profile is reconstructed by ionopsheric tomography method with the groun-GPS STEC measurements. The positions and lifetime of the observed red arc are not consistent with usual stable auroral red (SAR) arc, often observed as a red arc lasting for several hours in mid latitude regions during a magnetic storm. Instead, the observed red arc is consistent with a type of low latitude aurora with a lifetime of ~ 1 hr during the main phase of magnetic storm.

Mesosphere or Lower Thermosphere General Studies

MLTS-01 The nightglow measurements of the O2(0-0) atmospheric band by TIMED Doppler Interferometer (TIDI) - by Jong-Kyun Chung

Status of First Author: Non-student

Authors: J.-K. Chung, Q. Wu, S. Solomon, T. L. Killeen; HAO/NCAR, Boulder, CO, USA, D.A. Ortland; Northwest Research Associates, WA, USA, R. J. Niciejewski, W.R. Skinner; Space Research Laboratory, The University of Michigan, Ann Arbor, USA

Abstract: Limb scanning measurements of the O2(0-0) Atmospheric band emission by the TIDI instrument aboard the TIMED satellite during 2003-2005 are analyzed to examine their emission brightness variations according to the solar and geomagnetic activities. The data are restricted at latitudes 60S - 60N to avoid the contributions by the auroral emission. The variation of the nightglow brightness in latitude and local time is summarized in the yaw periods. The nightglow emission observed at LT = 21:00 - 03:00 are contoured on the geographic map to see their longitude-latitude distributions. The vertical emission profiles of the O2(0-0) Atmospheric band nightglow averaged in the 10 degree latitude range are investigated.

MLTS-02 The Numerical Modeling of Gravity Wave Packet Ducted due to the Thermal Structure in the Upper and Lower Atmosphere - by Yonghui Yu

Status of First Author: Student NOT in poster competition, PhD

Authors: Yonghui Yu, Physical Science Department, Embry Riddle Aeronautical University, Daytona Beach, Florida, and Physics Department, University of Central Florida, Orlando, Florida, U.S.A.
Yonghui.Yu@erau.edu
Michael P. Hickey, Physical Science Department, Embry Riddle Aeronautical University, Daytona Beach, Florida,
Michael.Hickey@erau.edu

Abstract: A time-dependent and fully nonlinear numerical model is employed to solve the Navier-Stokes equations in two spatial dimensions, and to describe the characteristics of a Gaussian gravity wave packet originated from the troposphere. Fourier analysis is used to analyze the frequency-dependent power spectrum of the wave packet propagating through and dwelling within the thermal duct regions. The frequency spectrum of the wave packet is derived at several discrete altitudes that allows us to determine the evolution of the packet. In addition we determine the horizontally-averaged vertical component of the wave energy flux and the horizontally-averaged wave kinetic energy density. Examination of these diagnostic variables allows us to better understand the process of wave ducting in the thermal duct of the lower thermosphere. The simulations also clearly reveal the existence of the stratospheric duct and the duct lying between the tropopause and the lower thermosphere. In all these cases wave kinetic energy is observed to reside in the ducts, while energy flux is seen to alternate in sign associated with the reflections of the wave between the duct's lower and upper boundaries. The spectral analysis allows us to unambiguously identify the ducted modes. These results compare favorably with those derived from our full-wave model.

MLTS-03 A study of negative ions in the D-region using ISR at Arecibo - by Shikha Raizada

Status of First Author: Non-student PhD

Authors: S. Raizada, M. Sulzer, C.A. Tepley, and S. Gonzalez

Abstract: Negative ions in the D-region govern the overall balance between production and loss, and hence modify the equilibrium electron density. Thus, knowledge of the negative ion to electron ratio is very important in understanding the complex behavior of the Dregion, and will help to validate current models. Theoretical studies have demonstrated that the presence of negative ions result in an increased ion line spectral width beyond
that expected for a given ion-neutral collision frequency, and this was confirmed by incoherent scatter radar measurements of the D-region from Arecibo. However, the broadening of spectral width can also result from other artificial interference like contamination from sources such as ships, airplanes, etc., which makes the D-region
difficult to study. Recently, we initiated incoherent scatter measurements of the ionospheric D-region with improved spectral resolution. For this experiment, we recorded every pulse, which helps us to eliminate interference that can increase the spectral width, and allows us to perform other statistical studies. A preliminary analysis of the recent data reveals a broadening of the spectral widths below 72 km altitude, near noon, which is consistent with previous measurements that were made nearly three decades ago. Those earlier results also reported the widths to broaden at altitudes higher than 80 km during the evening, which is not evident in the current data set.

MLTS-04 Mesosphere and lower thermosphere wind and turbulence observations over Puerto Rico during the Coqui 2 campaign - by Tianyu Zhan

Status of First Author: Student NOT in poster competition, PhD

Authors: T. Zhan (1), M. F. Larsen (1), J. H. Hecht (2)
(1) Clemson University, Clemson, South Carolina, USA, (2) The Aerospace Corp., Los Angeles, California, USA

Abstract: As part of the Coqui 2 sounding rocket campaign that was carried out in Puerto Rico in February and March 1998, a series of three rocket launches released the chemical tracer trimethyl aluminum (TMA) to measure the neutral wind profiles and turbulence structure in the mesosphere and lower thermosphere. The first launch was on February 19 when a sodium sudden atom layer was present and the other two launches were on the night of February 24/25 when enhanced gravity wave activity was detected in lidar measurements from the Arecibo Observatory and in ground-based imager data. The TMA trails were released on the upleg and downleg portion of each of the flights covering the altitude range from 85 to 150 km, thus providing measurements of the horizontal neutral wind velocities, as well as the gradients in the winds along a north/south direction. Large winds and wind shears were found between 95 and 110 km, which is a common feature of the wind profile at midlatitudes. The poster will focus

on the turbulent structure information obtained from the trails in combination with the measurements of O density profiles from on-board photometers, and the relation to the large winds and wind shears will be examined.

MLTS-05 Seasonal Investigations of Variance in Mesospheric Wave Structures at Low Latitudes - by Hema Karnam Surendra Babu

Status of First Author: Student IN poster competition, PhD

Authors: H. Karnam Surendra Babu, M. J. Taylor
Center for Atmospheric and Space Sciences and Physics Department, Utah State University.
J.H. Gunther
Department of Electrical and Computer Engineering, Utah State University.

Abstract: As a part of the Maui-MALT program, the Utah State University CEDAR Mesospheric Temperature Mapper (MTM) has operated continuously at Maui-Hawaii since November 2001. Over 1000 nights of high quality data on Mesospheric temperatures using the near infra red OH and O2 emission layers (centered at 87 and 94 km respectively) have been obtained over the past four years. In this study, we have analyzed data from 2003 (295 nights) to perform an initial investigation of the variance in OH and O2 signal as a function of wave periodicity. This was done by spectrally filtering the data into selected bands (approximately 1 hour wide). The data have been used to study variability in wave content on a night-to-night as well as a seasonal basis. Short period (10 min- 1 hour) waves were present throughout the year and indicate no obvious summer to winter difference in wave power. On sporadic nights throughout the year, both OH and O2 show remarkable enhancements of wave power (factor of 10). Here, we present the results of this initial study.

MLTS-06 A Global perspective of mesospheric inversion layers - by Ruth S. Lieberman

Status of First Author: Non-student

Authors: Ruth S. Lieberman, Dennis M. Riggin, R. L.
Collins, R. S. Stockwell and P. M. Franke

Abstract: Mesospheric inversion layers (MILs) are a ubiquitous feature of the mesosphere and lower thermosphere (MLT). MILs provide long-lived, planetary-scale environments for the ducting and trapping of upward-propagating gravity waves. Most MIL observations are obtained from measurements by Rayleigh and sodium light-detection systems. The resulting temperature profiles provide single-point perspectives of the juxtaposition of local and planetary-scale features. Satellite platforms provide near-global MLT coverage, and the ability to decompose the zonal wavenumber structure of the temperature field. Spacecraft whose orbits precess in local time provide further opportunities to examine the influence of tides upon MILs. We present global, seasonal and local-time dependencies of MILs as seen in TIMED SABER temperatures. We also show examples of how satellite data can aid in interpretation of point and "all-sky" measurements of MILs.

MLTS-07 Modeling study of airglow response to gravity wave perturbations in multiple layers in the mesopause region - by Fabio Vargas

Status of First Author: Student IN poster competition, Masters

Authors: Fabio Vargas - fabio@uiuc.edu, Gary Swenson - swenson1@uiuc.edu, Alan Liu - liuzr@ad.uiuc.edu

Abstract: Because gravity waves carry large amount of energy and momentum fluxes into the mesopause region, measurements of these fluxes are very important. In this work, simulations of the response of airglow layers to gravity wave perturbation were carried out based in the linear theory of gravity waves, photochemical models for the volume emission rate for airglow OH, O2 and O(1S), and background atmospheric model MSIS00. The cancellation factor for intensity and weighted temperature, the phase difference and the intensity amplitude ratio between layers were calculated. We also estimated the momentum and energy fluxes as well as the fluxes convergences between airglow layers due to dissipative gravity waves. The model results show good agreement with observational data.

MLTS-08 Investigating the horizontal characteristics of the short period gravity waves over Bear Lake Observatory, Utah - by Deepak Babu Simkhada

Status of First Author: Student IN poster competition, PhD

Authors: Deepak B. Simkhada and Mike J. Taylor, Center for Atmospheric and Space Sciences, Department of Physics, Utah State University, Logan, UT 84322, USA.
dbsimkhada@cc.usu.edu
mtaylor@cc.usu.edu

Abstract: Abstract. Based on airglow imaging data measured during 2002 at Bear Lake Observatory, Utah, the characteristics of small-scale gravity waves is investigated. These waves typically have short periods (7-12 min) with short horizontal wavelengths (8-35 km) and horizontal phase speeds of (20-55 m/s). The horizontal propagation directions in summer are either northeastward or northwestward, whereas, in winter the propagation directions are northwestward and southwestward. Most of the wave events with horizontal wavelengths of larger than 15 km are bands type, and the wave events of wavelengths smaller than 15 km are ripples type. These results indicate that the bands type waves are propagated from the lower atmosphere to the airglow heights in the mesopause regions.

Mesosphere and Lower Thermosphere Gravity Waves

MLTG-01 Gravity wave momentum flux estimated from airglow images in the equatorial mesopause region - by Shin Suzuki

Status of First Author: Student IN poster competition, PhD

Authors: Shin Suzuki (shin@stelab.nagoya-u.ac.jp), Kazuo Shiokawa, Yuichi Otsuka, and Tadahiko Ogawa, Solar-Terrestrial Environment Laboratory, Nagoya University, Minoru Kubota, National Institute of Information and Communications Technology, Takuji Nakamura, Research Institute for Sustainable Humanosphere, Kyoto University

Abstract: We developed a code to estimate vertical fluxes of horizontal momentum carried by small-scale (< 100 km) atmospheric gravity waves from OH airglow images in the mesopause region (80-90 km). Propagation direction, horizontal wavelength, horizontal phase speed, and intensity perturbation of gravity waves are estimated from the two-dimensional cross-power spectrum of two sequential time-differenced images, by a procedure similar to that developed by Tang et al. [IEEE Trans, pp. 103-109, 2005]. We also performed a process to remove the Milky Way structure from the airglow images. With these parameters and the cancellation factor introduced by Swenson and Liu [JGR, pp. 6271-6294, 1998], momentum flux is estimated from the polarization relations of gravity wave. We applied the method to the airglow images obtained at Kototabang, Indonesia (0.2S, 100.3E) for 26 nights from October 2002 to June 2005. The background wind data, which were essential for deriving the intrinsic parameters of gravity waves, were simultaneously measured by a meteor radar at Kototabang. Almost all gravity waves we extracted from airglow images had horizontal wavelengths of 30-60 km, apparent phase speeds of 30-70 m/s, and intensity perturbations of less than 2.0%. The momentum flux averaged over all the gravity wave events is 1.4 m2/s2. In the Asian monsoon season (June-August), some of wave components carried larger momentum than other seasons.

MLTG-02 Regional case study on the viability of short-range forecasting of convectively-generated gravity waves in the tropics - by Alexander Hassiotis

Status of First Author: Student IN poster competition, PhD

Authors: Jadwiga Richter and Tim Kane

Abstract: A regional case study is presented to investigate the feasibility of projecting the timing, location, and characteristics of convectively generated gravity waves in the tropics on short time scales. The gravity wave source spectrum will be prescribed based on 3-hourly coarse NCEP forecast fields. Limitations of this approach will be investigated using a high-resolution (~1-2 km) configuration of the WRF mesoscale model to explicitly compute the gravity wave spectrum above the convection. Results from this study will contribute to assessing the wave driving of the middle and upper atmosphere by waves generated from convective sources in the troposphere.

MLTG-03 On sodium measurements of gravity-wave momentum fluxes and assessment of gravity-wave/tidal interactionsOn sodium measurements of gravity-wave momentum fluxes and assessment of gravity-wave/tidal interactions - by Phillip Edward Acott

Status of First Author: Student IN poster competition, PhD

Authors: P. E. Acott, CSU, acott@lamar.colostate.edu, D. A. Krueger, CSU, krueger@lamar.colostate.edu, C. Y. She, CSU, joeshe@lamar.colostate.edu, B.P. Williams, CoRA, biff@cora.nwra.com, D. C. Fritts, CoRA, dave@cora.nwra.com

Abstract: Observation of gravity wave breaking and how it changes the zonal momentum flux budget in the mesosphere and lower thermosphere (MLT) is crucial to a better understanding of how gravity wave dynamics contribute to the global meridional circulation and temperature structure. Improvements underway at the Fort Collins CSU sodium lidar enable zonal momentum flux measurements while simultaneously measuring winds and temperature. These improvements coupled with the capability of doing 24-hour measurements will lead to a deeper understanding of the gravity wave/tidal interaction contribution to momentum flux divergence. Recent momentum flux measurements with the ALOMAR Weber sodium lidar system will be presented along with a discussion of the possible resolution at both ALOMAR and Fort Collins observatories.

MLTG-04 Incoherent Scatter Radar and All-Sky Imager Observation of Mesopsheric Gravity Waves at Arecibo - by Qihou Zhou

Status of First Author: Non-student

Authors: Zhou, Qihou; Y. T. Morton; Miami University
N. Aponte, Arecibo Observatory
S. Smith, Boston University

Abstract: Dual beam incoherent scatter radar observations have been carried out at Arecibo during the summer and winter. There is a strong seasonal variation between the two seasons. At about 75 km, gravity waves having a period of about 10-15 min during the day were ubiquitous in the summer while they are far less frequent in the winter. Gravity wave events in the summer are always associated with westward background wind and their vertical wavelengths are often very large. These waves are likely Doppler ducted. We further present the nighttime all-sky imager results.

MLTG-05 Photochemical-dynamical modeling of multi-layer airglow modulation by mesospheric gravity waves - by Jonathan Snively

Status of First Author: Student NOT in poster competition, PhD

Authors: J. B. Snively (jbs231@psu.edu)
V. P. Pasko (vpasko@psu.edu)

Abstract: Observations of multiple airglow emission layers, including the OH NIR Meinel, OI 557.7 nm, Na 589 nm, and O2 atmospheric bands, are used extensively in ground-based monitoring of gravity wave activity. With each emission layer arising at its respective altitude [e.g., Taylor et al., JGR, 102(D22), 26283, 1997], comparisons between measured emissions from different layers allow estimation of gravity wave vertical structure and wave properties [Liu and Swenson, JGR, 108(D4), 4151, 2003]. Interpretation of airglow data is contingent upon proper understanding of the airglow response to gravity waves. Similarly, interpretation of dynamical simulation results requires accurate modeling of photochemistry so that it may be compared with observations.

A new numerical model for the simulation of gravity wave-induced airglow modulation is presented. This model couples a fully-nonlinear, high-resolution, gas dynamics model [Snively and Pasko, GRL, 24, 2254, 2003, and references cited therein] with airglow photochemical models for the OH and OI airglow emissions based upon work by Makhlouf et al. [JGR, 100(D6), 11289, 1995] and Makhlouf et al. [JGR, 103(D6), 6261, 1998], respectively, while adopting several assumptions to reduce computational expense. The dynamical model accounts for nonlinear transport of relevant minor and major species due to nonlinear gravity wave motions, in addition to simple diffusive processes.

Airglow modulation by short-period ducted gravity waves is examined for the simple cases of Doppler and thermal ducting near mesopause altitudes. Results are compared with existing numerical models [e.g., Snively and Pasko, GRL, 32, L08808, 2005 and references cited therein], which rely extensively upon steady-state assumptions and empirical parameters. Additionally, simplified models for O2 atmospheric bands [Murtagh et al., PSS, 38(1), 42, 1990, and references cited therein] and Na 589 nm emissions

[Swenson and Gardner, JGR, 103(D6), 6271, 1998] are presented to allow comparison between the four commonly-observed airglow layers under realistic model conditions.

MLTG-06 Lidar study of gravity waves and their influence on polar mesospheric clouds in Antarctica - by Chihoko Yamashita

Status of First Author: Student IN poster competition, Masters

Authors: Chihoko Yamashita1, Xinzhao Chu1, Graeme Nott2, Patrick Espy3
1 Department of Aerospace Engineering Science, University of Colorado at Boulder, USA
2 Department of Physics and Atmospheric Science, Dalhousie University, Halifax, Canada
3 Physical Sciences Division, British Antarctic Survey, Cambridge, UK

Abstract: Gravity waves play an important role in the dynamics of global middle and upper atmosphere. It has been suggested that gravity waves may influence the formation or occurrence of polar mesospheric clouds (PMC). An initial study using Rayleigh lidar at Greenland (67.0° N, 50.9° W) indicates that the strength of gravity waves and PMC are negatively correlated. However, such a correlation has not been examined in Antarctica until now. Extensive lidar data of PMC and relative atmosphere density were obtained at Rothera (67.5° S, 68.0° W), Antarctica from December 2002 to March 2005 with the University of Illinois Rayleigh/Fe Boltzmann lidar. This provides us a good opportunity to investigate the gravity waves and their influence on PMC in Antarctica. In this paper the root-mean-square (RMS) relative density perturbation derived from the Rayleigh lidar data is used to characterize the stratospheric gravity wave activities, while the total backscatter coefficients (TBC) are used to represent PMC events in the mesopause region. In order to show the relationship between gravity wave and PMC, the daily averaged TBC and RMS density perturbation vales are compared. The resulted linear correlation coefficient is -0.48within 95% confidence level. The RMS density perturbation error value of 0.14 is considered the geophysical variability and photon noise, and this may be the worst case error. In order to consider the error of each data point in the linear correlation coefficient results, we take the random value in the error range, run 10000 times, and take average (i.e., Monte Carlo method). In this case, the linear correlation coefficient is -0.33, and standard deviation is ±0.12. This result use the worst case error; however, in order to take more realistic value, we use 1/2 error value. In this case, the linear correlation coefficient is -0.43 within 95% confidence level with the standard deviation of ±0.07. The obtained correlation coefficient at Rothera is similar to the Arctic result of a linear correlation coefficient of -0.44 (from the actual data point) and -0.35 (using Monte Carlo method with 1/2 standard deviation) [Gerrard et al., 2002]. These results show that the stratospheric gravity waves have negative influence on PMC formation, i.e., larger gravity wave activities results in weaker PMC brightness.

MLTG-07 Propagation and Ducting of Short-Period Gravity Waves over Antarctica - by Kim Nielsen

Status of First Author: Student IN poster competition, PhD

Authors: K. Nielsen, and M.J. Taylor
Center for Atmospheric and Space Sciences (CASS), Physics Department, Utah State University.
M. J. Jarvis
British Antarctic Survey (BAS)

Abstract: Short-period gravity waves are known to be significant sources of momentum deposition in the upper mesosphere. Recent studies using an extensive imaging data set obtained as part of a collaborative program with British Antarctic Survey have identified significant differences in the momentum transported by short-period waves as observed from Halley Station (76°S, 27°W) on the Brunt ice shelf and Rothera Research Station (67° S, 68° W) on the Antarctic Peninsula. However, this result is recognized to be an upper limit since it assumes that all of the wave motions were freely propagating. In this study we utilized available mesospheric wind data from Halley to investigate the propagation nature (i.e. freely propagating, evanescent, or Doppler ducted) of these waves observed over Halley during the 2000 and 2001 austral winter seasons to help provide a more realistic assessment of the impact of short-period waves on the Antarctic environment (note: it was not possible to identify thermally ducted waves with the existing data set). A total of ~170 short-period wave events were observed with available coincident wind measurements. The majority of these waves were found to be freely propagating (~78%) with only ~3% of the observed events clearly Doppler ducted. In the remaining cases (21%), the mesospheric winds did not support propagating waves (evanescent).

MLTG-08 Short-period mesospheric gravity wave propagation and momentum flux at low-latitudes using simultaneous Na lidar and temperature mapper measurements - by Mitsumu K. Ejiri

Status of First Author: Non-student

Authors: M. K. Ejiri (1), M. J. Taylor (1), P. D. Pautet (1), Y. Zhao (1), K. Nielsen (1), and A. Z. Liu (2)
(1) Center for Atmospheric and Space Sciences, Utah State University, USA
(2) Department of Electric and Computer Engineering, University of Illinois at Urbana-Champaign, USA

Abstract: The US Maui-MALT program is designed to investigate the properties and dynamics of the low-latitude mesosphere and lower thermosphere region (MLT) in exceptional detail. A key component of this study is the investigation of short-period gravity waves and their propagation and dissipation characteristics at MLT height. High-resolution measurements of the background wind, temperature field using the University of Illinois Na wind/temperature lidar have been combined with simultaneous image measurements of the NIR OH and O2 airglow intensity and rotational temperature obtained by the Utah State University Mesospheric Temperature Mapper (MTM) to perform an in-depth investigation of five selected short-period (less than 20 min) gravity wave events. In each case, the waves were observed under differing background conditions and we have determined their intrinsic properties, and nature of propagation (i.e. freely propagating or ducted). This has allowed us to quantify their associated horizontal momentum fluxes at two different altitudes (87 and 94 km) within MLT.

MLTG-09 Investigaing mesospheric gravity waves and their potential role in seeding thermospheric depletions over Brazil - by Pierre-Dominique Pautet

Status of First Author: Non-student

Authors: Pierre-Dominique Pautet (pautet@cc.usu.edu),,Michael J. Taylor (mtaylor@cc.usu.edu), Utah State University, Logan, UT, USA, Dave C. Fritts (dave@cora.nwra.com), Northwest Research Institute, Inc., Boulder, Co, USA

Abstract: Atmospheric gravity waves propagating from the troposphere up to the lower thermosphere play a key role in the thermal structure and large-scale circulation of the mid-atmosphere. The NASA Living with a Star program supported a campaign in Brazil to study the effects of gravity waves on the ionosphere and particularly their role in the seeding of Rayleigh-Taylor instabilities, strong equatorial spread-F and plasma bubbles. Several US and Brazilian institutes involved in this project deployed a large range of instruments (all-sky imagers, digisondes, photometers, meteor/VHF radars, GPS receivers) to cover a large area of Brazil. The campaign was divided in two observational phases centered on the September and October new moon periods.

This poster summarizes the results obtained with the USU all-sky CCD imager operated at Sao Joao d'Alianca (14.75°S, 47.60°W). The data obtained during 17 clear nights have been studied to determine the characteristics of the short-period gravity waves observed at mesospheric heights. The results show two main directions of propagation (towards NE and SE) as well as the presence of several gravity wave events with wavelength greater than 100km that are thought to be more important for ionospheric seeding. The thermospheric structures observed in the 630nm emission will also be presented.

MLTG-10 Gravity Waves and Momentum Fluxes in the MLT Using 430 MHz Dual-Beam Measurements at Arecibo - by Diego Janches

Status of First Author: Non-student

Authors: D.C. Fritts, D.M. Riggin, R.G. Stockwell (NWRA/CoRA Div.)
M.P. Sulzer and S. Gonzalez (Arecibo Observatory)

Abstract: We report on a new use of the UHF radar at the Arecibo Observatory in Puerto Rico. We have employed the 430 MHz radar for incoherent scatter measurements of radial wind spectra at altitudes from ~71 to 95 km using the Gregorian and line-feed antennas to define two beams inclined 15 degrees to the east and west of zenith. We find that the two beams define radial velocities with sufficient accuracy to characterize both the gravity waves (GWs) and the momentum fluxes due to these waves over the majority of the observed altitude range during daylight hours. The characteristics of the GWs inferred from these measurements include 1) vertical scales ranging from ~2 to 20 km, 2) downward phase progression of the dominant GWs up to ~5 m/s, and 3) vertical wavenumber spectra having slopes near the value expected for saturated GWs. The coplanar, dual-beam experiment was specifically designed to test the ability to measure GW momentum fluxes and their frequency distributions. Radial velocity variances reveal preferential eastward propagation for most intervals and altitudes. The momentum fluxes observed during

this experiment had ~1-hr averages that were often near zero, occasionally achieved amplitudes of ~20 to 50 m^2/s^2, displayed significant consistency in altitude, and exhibited an approximate anti-correlation with the zonal wind field in cases with significant momentum fluxes. Frequency spectra defined the major contributions to the momentum fluxes, while S transforms were employed to examine the temporal variability of the GWs and momentum fluxes in greater detail.

MLTG-11 Observations of Wave Breaking and Mean Flow Acceleration - by Bob Stockwell

Status of First Author: Non-student

Authors: R.G. Stockwell(1), M.J. Taylor (2), K. Nielsen (2), M. Jarvis(3)

(1) Colorado Research Associates, Boulder, CO, USA,
(2) Center for Atmospheric and Space Sciences, Utah State University, Logan, Utah, USA,
(3) British Antarctic Survey, Cambridge, U.K.

Abstract: All-sky OH images of a breaking mesospheric wave packet have been made from Halley Station Antarctica (75.5 S, 26.7 W). Two dimensional S-Transform analysis is applied to calculate the wave's period, wavelength, phase speed and group speed. The bore theory is used to calculate the duct parameters depth and
it is shown that as the wave packet breaks, the bore duct collapses while simultaneously the background winds experience a large acceleration in the direction of the wave propagation.

Mesosphere and Lower Thermosphere Gravity Waves

MLTT-01 Joint Time-Frequency Representations of Large Geophysical Datasets - by Bob Stockwell
Status of First Author: Non-student

Authors: R. G. Stockwell
Colorado Research Associates Division,Northwest Research Associates Inc.,
Boulder, CO, USA.

Abstract: A orthogonal basis for the S-Transform (a joint time-frequency representation) is introduced that allows one to examine local spectral features of arbitrarily large datasets. These basis functions are defined to have phase characteristics that are directly related to the phase of the Fourier transform spectrum, and are both compact in frequency and localized in time. Distinct from a wavelet approach, this approach allows one to directly collapse the orthogonal local spectral representation over time to the complex-valued Fourier Transform Spectrum. Because it maintains the phase properties of the S-transform, one can perform Localized Cross Spectral Analysis and one can define a channel Instantaneous Frequency. This analysis is applied to several years of MF radar winds measured at Hawaii, USA.

MLTT-02 Study of an ion-drag contribution to the lower thermospheric wind in the summer polar cap using the ESR data - by Takuo Tsuda

Status of First Author: Student IN poster competition, PhD

Authors: T. Tsuda, S. Nozawa, A. Brekke, Y. Ogawa, T. Motoba, R. Roble, R. Fujii

Abstract: We have investigated the importance of the convection electric field (i.e., the ion-drag) on the lower thermospheric wind dynamics in the summer polar cap using the data obtained for the six consecutive days, from 1000 UT on July 1 to 1000 UT on July 7, 1999, with the EISCAT Svalbard Radar (ESR) located in Longyearbyen (78.2 deg N, 16.0 deg E). The electric field in the F region exhibited a stable diurnal variation lasting almost over the first three days of the observations, while the diurnal variation was not clearly identified for the latter three days. On the basis of the difference of the electric field variation, we divided the datasets into two intervals (three day length each) and compared the diurnal tidal amplitudes and phases between the two intervals. The amplitude of the meridional diurnal tide for the first three days was larger than that for the latter three days over the height region between 100 and 118 km. For the zonal component, the difference was small. The difference was interpreted by the ion-drag effect to some extent, indicating the ion-drag plays an important role in the neutral wind dynamics. In addition, we compared NCAR TIME-GCM predictions with the observations. The TIME-GCM predictions also indicated that the diurnal tide is influenced by the convection electric field.

MLTT-03 Structure of the Migrating Diurnal Tide in the Whole Atmosphere Community Climate Model - by Loren Chang

Status of First Author: Student IN poster competition, PhD

Authors: L. Chang, S.E. Palo; University of Colorado, Department of Aerospace Engineering Sciences
M. Hagan, J. Richter, R. Garcia; National Center for Atmospheric Research
D. Riggin, D. Fritts; Colorado Research Associates

Abstract: The migrating diurnal tide is a dominant and persistent feature of the middle and upper atmosphere, attaining amplitudes in excess of 10K in temperature and 30 m/s in the horizontal wind field at tropical latitudes. This oscillation, with a period of 24 hours and a wavenumber 1, propagates westward with the apparent motion of the sun and is forced from the absorption of solar radiation by water vapor in the troposphere and ozone in the stratosphere. As the tide propagates upwards it grows in amplitude, conserving energy, and transports heat and moment away from its source region in the troposphere and stratosphere. This heat and momentum is eventually deposited in the mesosphere and lower thermosphere thus effecting the zonal mean circulation of the region.
The NCAR Whole Atmosphere Community Climate Model (WACCM) is a comprehensive global circulation model that spans from the surface of the Earth into the lower thermosphere. It is the next generation model and includes self consistent physics from the surface through the lower-thermosphere. Version 3 of WACCM has been run for a year, and the migrating diurnal tide is extracted. In this presentation, we examine the migrating diurnal tide generated in WACCM, and compare with similar results generated by the Global Scale Wave Model (GSWM), a linear model derived from basic tidal theory; as well as with actual ground based tropical radar observations.
We find that WACCM correctly resolves the semiannual variation of the migrating diurnal tidal amplitude, which is one of the dominant long term features of the tide, as well as the basic spatial structure. However, the WACCM tidal amplitudes are clearly lower then in the GSWM, as well as most previous observations; possibly due to problems modeling tropospheric and stratospheric forcing. Additionally, a significantly larger degree of hemispherical asymmetry exists in the WACCM results, especially near solstice. We present and explore factors that may contribute to these differences; including forcing, dissipation, and the zonal mean zonal winds.

MLTT-04 An Intercomparison of Atmospheric Tidal Oscillations in the Horizontal Wind Field Observed over Antarctica - by Hiroyuki Iimura

Status of First Author: Non-student PhD

Authors: H. Iimura, S.E. Palo, J.M. Forbes, E.M. Lau, S.K. Avery, J.P. Avery, Yu.I. Portnyagin, N.A. Makarov, E.G.Merzlyakov, D.M. Riggin, D.C. Fritts, R.E. Hibbins, R.A. Vincent, D.J. Murphy, T. Aso, M. Tsutsumi, A.J. McDonald, and N.J. Mitchell

Abstract: The atmospheric tides are a dominant and persistent feature of the mesosphere and lower-thermosphere region of the atmosphere which spans from 80 to 120km above the Earth's surface. The tides, primarily forced through the absorption of water vapor in the troposphere and ozone in the stratosphere, propagate vertically transporting heat and momentum between the lower and upper atmosphere. Observations from a network of radars operating across the Antarctic continent are analyzed to determine the coherent spatial and temporal structures present in these tidal operations. Data includes observations from Rothera, Davis, Syowa, Sanae, Halley, Scott Base, McMurdo and South Pole. Analysis of the diurnal and semidiurnal tides from these sites are compared using multiple years of data to determine the annual structure of the tidal oscillations. These observations are compared with the Global Scale Wave Model (GSWM) in an effort to understand how the model reproduces the observations.

MLTT-05 Observations of Upper Mesospheric and Lower Thermospheric Temperatures and Winds using Ground-Based Airglow Measurements in the Low and High-Latitude - by Young-In Won

Status of First Author: Non-student

Authors: Young-In Won1, G. G. Sivjee1, S. M. Irfan Azeem1, Qian Wu2, Michael Kuss1, and Charles Mutiso1
1Department of Physical Science, Embry-Riddle Aeronautical University, 600 S. Clyde Morris Blvd., Daytona Beach, FL 32114
2HAO/NCAR, P.O.Box 3000, Boulder, CO 80307-3000

Abstract: Terrestrial nightglow emissions in the near infrared region have been measured in Daytona Beach (29.21º N, 81.04 º W), FL, U.S.A. and northern high latitude (Resolute Bay, 74.68º N, 94.90º W), Canada from ground-based optical instruments. Lower thermospheric and upper mesospheric temperature and wind information are derived from Michelson interferometer and Fabry-Perot Interferometer observations of OH Meinel bands and OI (557.7 nm) emission to study the periodicities of the

atmospheric waves. The amplitudes and phase information of the major oscillations from two different locations are calculated and compared.

Meteor Science other than Wind Observations

METR-01 Modeling the Meteoric mass deposition in the Upper Atmosphere - by Amal Chandran
Status of First Author: Student IN poster competition, PhD

Authors: Amal Chandran, Department of Aerospace Engineering Sciences, University of Colorado, Boulder, Co
Diego Janches, NorthWest Research Associates, Colorado Research Associates Division, Boulder, Co
Scott Palo, Department of Aerospace Engineering Sciences, University of Colorado, Boulder, Co

Abstract: It is now widely accepted that sporadic extraterrestrial particles in the size range of 10-11 to 104 g are likely to be the major contributors of metals in the Mesosphere/Lower Thermosphere (MLT). It is also well established that this material gives rise to the upper atmospheric metallic and ion layers. In addition, micrometeoroids are an important source for condensation nuclei (CN), the existence of which is a prerequisite for the formation of NLC particles in the polar mesopause region. In order to understand how this flux gives rise to these atmospheric phenomena, accurate knowledge of the global meteoric input function (MIF) is critical. This function accounts for the annual and diurnal variations of meteor rates, global distribution, directionality, and velocity and mass distributions. Recently, Janches et al. (Modeling the Global Micrometeor Input Function in the Upper Atmosphere Observed by High Power and Large Aperture Radars, JGR, In print, 2006) showed that in order to obtain agreement between modeled and observed diurnal and seasonal variability of the meteor rate at three different geographical locations, an empirical atmospheric filtering effect needs to be taken into account. This empirical filter prevents meteors with low elevation radiants (< 200) from being detected by the radars at mesospheric altitudes. In this poster, we present modeling results of the meteoroid atmospheric entry processes in order to understand the origins of this atmospheric effect and to properly calculate how and where meteoric mass is deposited in the upper atmosphere. The modeled processes include meteoroid ablation, electron production, heating and deceleration which are caused by the interaction between meteoroids and the air molecules. As shown by the results, these processes are highly dependant on meteor parameters such as mass, density, size, velocity and entry angle. We also present comparisons between modeled and observed meteor head-echo altitude distributions. This is the first time such comparisons are made. The observations were obtained with the 430 MHZ Arecibo radar. This comparison, which shows reasonable agreement, was performed by assuming that a minimum electron density is required to be produced for radar detection.

METR-02 Processing algorithms for meteor-head characterization over Jicamarca - by Freddy Ronald Galindo

Status of First Author: Student NOT in poster competition, Undergraduate

Authors: F. Galindo and J.L. Chau

Abstract: The main problem for studying meteor-head echoes over Jicamarca (11.95° S, 76.87° W) is the presence of coherent echoes due to the Equatorial Electrojet (EEJ). They are generated at the same altitudes that the meteor-head echoes (around 100 km of altitude). The first experiments to study meteors were done around sunrise, because at this time the EEJ echoes are usually very weak or absent. These datasets were originally processed with an automated processing scheme [Chau and Woodman, 2004]. Such algorithm detected and characterized many meteor heads, but it was very conservative, for example, no meteor-heads were considered when EEJ echoes were present.
In this poster we present a new processing algorithm where the detection of meteors is done manually. Such detection is done with a simple user-friendly graphical user interface (GUI). After each possible meteor is detected all the meteors parameters are estimated and depending on those values, a meteor is accepted or not. This new algorithm allows us to select meteors which occur at different altitudes from the EEJ, those occurring at the same time but different altitudes, and, when the meteor-head echoes are strong enough, meteors are detected in the presence of EEJ echoes. In addition, few schemes dealing with EEJ echoes are presented. Such schemes could be used in the future for implementing an automated but aggressive detection.

METR-03 A Comparison Of Automated-Search Meteor Results From Radar Observations At Two Locations - by Stanley Briczinski

Status of First Author: Student IN poster competition, PhD

Authors: S.J. Briczinski <sjb144@psu.edu>, J.D. Mathews <jdmathews@psu.edu>, D.D. Meisel <meisel@geneseo.edu>, C.J. Heinselman <craig.heinselman@sri.com>

Abstract: The automated FFT periodic micrometeor searching algorithm developed by Mathews et al. [An update on UHF radar meteor observations and associated signal processing techniques at Arecibo Observatory, JASTP 65 (2003) 1139-1149] has now cataloged over 33,000 separate sporadic meteor events seen with the 430 MHz Arecibo Observatory radar over 30 hours of observation time. An additional 30 hours of meteor data were taken in July and August 2005 using the 1290 MHz Sondrestrom incoherent scatter radar. The Sondrestrom radar was run in two modes to observe sporadic meteors. In the first mode, the radar beam was pointed at zenith to mimic conditions at Arecibo. In the second mode, the radar beam was pointed due east at an 85 degree zenith angle. The second configuration was chosen as an attempt to maximize the meteor flux rate and is an observation condition not possible using the Arecibo radar. The searching algorithm was run on data sets from both radars. We present and compare sporadic meteor parameters (i.e. altitudes, velocities, decelerations) from both facilities while considering the resultant insights into the head-echo scattering process at 430 MHz versus 1290 MHz. We also use the observation parameters to determine mass distributions.

METR-04 Analysis of the Leonid Meteor Shower using a VHF interferometric Meteor Radar - by Santiago de la Peña

Status of First Author: Student IN poster competition, PhD

Authors: Susan K. Avery , James P. Avery

Abstract: Every year the earth crosses or passes near one of the dust trails left by comet Tempel - Tuttle in its pass through the solar system every 33.2 years. This produces a meteor shower commonly called the Leonid. The 2001 Leonid meteor shower is one of the strongest in recent years. We present data collected by the 50 MHz all-sky meteor radar located at Platteville, CO, with a discussion of the intensity of the phenomena, a methodology for the estimation of the radiant flux of the meteor shower and estimates of the meteor mass indexes for the duration of the shower.

METR-05 Antenna pattern measurement using radio stars - by Vijay Subbaraman Venkatesh

Status of First Author: Student IN poster competition, Masters

Authors: James Avery
Department of Electrical Engineering
University of Colorado, Boulder.
email: james.avery@colorado.edu

Abstract: The sizes of antennas at lower VHF frequencies makes it impractical to have their pattens measured in anechoic chambers. Consequently, methods employing radio stars have grown popular. In this poster, the method shown involves measuring the received power levels, with the intention of correlating the differences in received power from celestial bodies such as the sun and the antenna pattern. The antenna of interest is the receive antenna array of the 40 MHz MEDAC system at Platteville,CO.

METR-06 High range-resolution meteor observations from the Jicamarca Radio Observatory - by Elizabeth Bass

Status of First Author: Student IN poster competition, PhD

Authors: Elizabeth Bass (enb@bu.edu), Meers Oppenheim (meerso@bu.edu), Jorge Chau

Abstract: High-power, large-aperture (HPLA) radars observe two signatures of meteors: head echoes and non-specular trails. In July 2005, new HPLA observations were taken using the 50MHz antenna at the Jicamarca Radio Observatory in Peru. Thousands of head echoes and hundreds of trails were detected during the five hours of measurements. A sub-microsecond pulse period was used to provide maximum resolution in both time and range. Three different phase and amplitude signals were received from separate quarters of the radar, allowing high precision interferometry. This poster will present a sample of the observed head

echoes and their 3-D positions and velocities. The combination of high range-resolution, interferometry, and Doppler should allow us to accurately estimate meteor mass and evaluate sample biases, further characterizing the meteor population.

METR-07 Observations of Inertia-gravity wave from long-lasting meteor trail echo with hodograph analysis - by Chao-Tuan Cheng

Status of First Author: Student NOT in poster competition, PhD

Authors: Chao-Tuan Cheng, Institute of Space Science, National Central University, Chung-Li, Taiwan.
Yen-Hsyang Chu, Institute of Space Science, National Central University, Chung-Li, Taiwan.

Abstract: Mesospheric horizontal winds deduced from the drift of long lasting meteor trail were investigated in this paper. The meteor trail was positioned by using interferometry technique implemented at the Chung-Li VHF radar. The height variation of the horizontal wind velocity was estimated from the drift of the meteor trail lasting more than 23 seconds lasting in height region between 95 and 108 km . Hodograph method was applied to the analysis of the horizontal wind velocity profile and the result showed that the wind vectors rotated clockwise with increase of heights. This feature strongly indicates existence of upward propagating inertia-gravity wave. The characteristics of the gravity wave are that the intrinsic period is about 6 hours, the vertical wave length is 11.3 km and the horizontal wave length is 1038 km. The observed vertical wind shear combined with the Brunt-Vaisala frequency of MSIS model was used to estimate the height variation of the Richardson number Ri. We found that $Ri < 0.25$ in height range 98 to 99 km. This result implies that the wave is vary liking to be broken in this height region, and the wave-breaking turbulences presumably induce the corresponding plasma irregularities in the meteor trail.

Sprites

SPRT-01 Sprite spectra at high time resolution - by Takeshi Kammae
Status of First Author: Student IN poster competition, PhD

Authors: T. Kammae and H.C. Stenbaek-Nielsen, Geophysical Institute, University of Alaska Fairbanks
tkammae@gi.alaska.edu
M. G. McHarg, US Air Force Academy

Abstract: Sprite spectra were recorded with an imaging spectrograph with 3 ms and 3 nm temporal and spectral resolution respectively. The spectral coverage was 640 nm to 830 nm. The slit was vertical so that altitude variations can be resolved. The observations were made from Langmuir laboratory, New Mexico, in July, 2005. The spectra are dominated by the N2 1PG bands. There is no or little evidence of the N2+ Meinel band structures in the observed spectra. This is in agreement with calculated spectra.
The N2(B) vibrational distribution varies in altitude and becomes similar to that of laboratory afterglow from tendrils as suggested by Bucsela et. al[1]. This suggests that some N2(B) excitation processes other than simple electron impact may play a role, especially in the tendrils. [1] Bucsela et al., 2003, Journal of Atmospheric and Solar-Terrestrial Physics, 65, 583-590

SPRT-02 On the OH Nightglow Emission in the Occurrence of Sprites - by Tai-Yin Huang

Status of First Author: Non-student

Authors: T.-Y. Huang and Steven Troxell
Physics Department, The Penn State University Lehigh Valley, Fogelsville, PA 18051, USA. tuh4@psu.edu

Abstract: Previous simulations of the OH nightglow emission in the occurrence of sprites by Huang [2005] have indicated that the column-integrated OH intensity would be enhanced significantly when sprites occur. The chemical reactions were taken from Walterscheid et al. [1987], in which they only considered OH ground state. Recent simulations using a different but more complete set of OH chemical reactions from Hickey et al. [2003] have revealed that an even more significant increase in the column-integrated OH brightness would result in the occurrence of sprites. The major difference between the two chemical reaction sets is that the latter includes OH excited states in the reactions. Comparisons between the two model simulation results will be discussed.

SPRT-03 Lightning Sprite Relationship With High Time Resolution Analysis - by Jingbo Li

Status of First Author: Student IN poster competition, PhD

Authors: Li, J., Cummer, S. A., Jaugey, N., Department of Electrical and Computer Engineering, Duke University, Durham, NC 27708
Lyons, W. A., Nelson, T. E., FMA Research, Inc., Yucca Ridge Field Station, Ft. Collins, CO 80524
Gerken, E. A., Center for Geospace Studies, SRI International, Menlo Park, California, 94025

Abstract: Through simultaneous measurements of high altitude optical emissions and the magnetic field produced by sprite associated lightning discharge, previous studies have uncovered many aspects of the relationship between these phenomena. However, few data sets have acquired both of these measurements with the millisecond or faster time accuracy and resolution on which many sprite-associated phenomena occur. In this work, we report results of the coordinated analysis of high speed sprite video and wideband (0.1 Hz to 30 kHz) magnetic field measurements made simultaneously at the Yucca Ridge Field Station and Duke University during the June through August 2005 campaign period. The absolute time accuracy and precision of all instruments has been verified on the order of 10 microseconds, and the intensified high speed video was acquired at rates between 1000 and 10000 frames per second. These data thus enable a close examination with high time resolution of the link between low altitude lightning processes and high altitude sprite processes. We similarly investigate the relationship of lightning charge transfer characteristics and long delayed (>100ms) sprite morphology and duration, which is still not well understood yet. On one observation night (4 July 2005), a large mesoscale convective system produced many sprites that were part of complex TLE sequences that included optical emission elements that appear well after any return stroke and initiate at apparently relatively low altitudes. The connection between these elements and the complex temporal structure of the underlying lightning flash as observed with the magnetic sensors is discussed.

SPRT-04 Modeling Studies of Initiation and Propagation of Sprite Streamers - by Ningyu Liu

Status of First Author: Non-student PhD

Authors: Ningyu Liu (nul105@psu.edu) and Victor Pasko (vpasko@psu.edu)
The Pennsylvania State University, Communications and Space Sciences Laboratory, University Park, PA 16802

Abstract: Sprite discharges represent one of four known types of transient luminous events occurring in the Mesosphere and Lower Thermosphere-Ionosphere (MLTI) regions, which are directly related to the lightning activity in underlying thunderstorms. Although a typical sprite event may occupy a large overall volume of the upper atmosphere, high spatial resolution imagery of these events reveals many internal and not yet fully understood small-scale features, including bright filamentary channels of ionization [Gerken and Inan, IEEE Trans. Plasma Sci., 33, 282, 2005, and references therein]. It is quite remarkable that the filamentary structures observed in sprites are the same phenomenon known as streamer discharges at atmospheric pressure, only scaled by reduced air density at higher altitudes [e.g., Liu and Pasko, JGR, 109, A04301, 2004].

The relationship of streamers at different pressures is guided by similarity relations [e.g., Roth, Industrial plasma engineering, Vol. 1, 1995, p. 306], which represent a useful tool for analysis of gas discharges since they allow to use known properties of the discharge at one pressure to deduce features of discharges at variety of other pressures of interest, at which experimental studies may not be feasible or even possible. Streamer discharges similar to those documented in sprites [Gerken and Inan, IEEE Trans. Plasma Sci., 33, 282, 2005, and references therein] have been observed in point-to-plane discharge geometry in laboratory experiments at near ground pressures [Pancheshnyi et al., Phys. Rev. E, 71, 016407, 2005; Briels et al., IEEE Trans. Plasma Sci., 33, 264, 2005]. Understanding of the physical processes which lead to the observed departures from similarity relations at different pressures in these experiments represents an important problem, resolution of which would synergistically benefit understanding of streamers in both systems (i.e., due to generally relaxed requirements on time resolution of imaging systems needed for studies of sprite streamers, and easy repeatability of discharges in high pressure laboratory experiments). In this talk we report results from a streamer model developed in [Liu and Pasko, JGR, 109, A04301, 2004; GRL, L05104, 2005; J. Phys. D: Appl. Phys., 39, 327, 2006] as applied to propagation of positive streamers at various pressures in air in a point-to-plane discharge geometry. We directly compare our results with recent experiments at atmospheric and near atmospheric pressures in air reported in [Pancheshnyi et al., 2005; Briels et al., 2005]. We will also discuss the implications of our modeling results for interpretation of the most recent high-speed imaging of sprites which demonstrates that the visible sprite streamer channels in normal rate video are formed by the rapid propagation of glowing streamer heads [McHarg et al., Eos Trans. AGU, 86(52), Fall Meet. Suppl., Abstract AE11A-04, 2005; Stenbaek-Nielsen et al., Program and Abstracts, p. 282, URSI National Radio Science Meeting, 2006], and that sprite streamers may initiate from brightening inhomogeneities at the bottom of a sprite halo, an amorphous diffuse glow formed at the lower ionosphere following lightning flashes [Cummer et al., GRL, 33, L04104, 2006].

SPRT-05 Infrared Imaging of Transient Luminous Events (1 - 1.5 micron) Over the Mid-Western US and Comparison With Their Visible Wavelength Signatures - by Matt Bailey (presented by Michael Taylor)

Status of First Author: Student NOT in poster competition, PhD

Authors: Matt Bailey, Michael J. Taylor, Dominique Pautet, Center for Atmospheric and Space Sciences and Physics Department, Utah State University;
Walter A Lyons, FMA Research Inc.;
Steven Cummer, Department of Electrical and Computer Engineering, Duke University

Abstract: As part of a coordinated campaign conducted from Yucca Ridge, Colorado, during summer, 2005, four sensitive imaging systems were fielded by Utah State University to investigate the signatures of transient luminous events (TLEs) over a broad spectral range, extending from the near ultra violet (0.35 microns) to infrared wavelengths (1.5 microns). These measurements were made in conjunction with high speed video and electromagnetic observations providing detailed information of the TLE dynamics and their structures. The USU instruments consisted of two GEN. 3 Xybion cameras, one filtered to observe N2 first positive emissions (665 nm) while the second observed white light emissions. A third intensified camera with an extended blue response was fitted with a broad band filter to observe the N2+ first negative and N2 second positive emissions (band width, 350 - 475 nm). Novel infrared measurements were made using an InGaAs imaging array operating at video rates. All four cameras had similar field of view (25 degrees) and were co-alligned on a single mount with the high speed imager. We discovered that sprites were easily imaged in the infrared spectral range, and over 30 events were captured with the InGaAs camera arising from thunderstorms over the mid-western United States during early July through mid August. This poster presents new measurements of the optical characteristics of TLE's imaged in the infrared spectral range (1 - 1.5 microns) and an initial comparison with their visible and near UV signatures.

SPRT-06 Evidence for direct cloud-to-ionosphere electrical connection through sprite and jet processes - by Robert Andrew Marshall

Status of First Author: Student IN poster competition, PhD

Authors: Robert A. Marshall, STAR Laboratory, Stanford University, ram80@stanford.edu
Umran S. Inan, STAR Laboratory, Stanford University, inan@stanford.edu

Abstract: We report on a class of sprite observations over the Southwest United States that show evidence of connection to the parent thundercloud. In each event, a large sprite is observed in the usual altitude range (~40 to 90 km), but at the peak of its development, a jet-like structure appears, that seems to propagate from the cloudtop to the base of the now-fading sprite. Such events have been previously reported but never explained in the context of their impact on the cloud-ionosphere connection. Furthermore, we report photometric and ELF/VLF data that support the conclusion of a direct cloud-to-ionosphere electrical connection.

Extraterrestrial Planetary Atmosphere

EPAT-01 Saturn's Ionosphere: Cassini Radio Occultation Measurements and Model Comparisons - by Luke Moore

Status of First Author: Student IN poster competition, PhD

Authors: Luke Moore, Michael Mendillo, Boston University
Andrew F. Nagy, University of Michigan
Arvydas J. Kliore, California Institute of Technology / JPL
Ingo Mueller-Wodarg, Imperical College
John D. Richardson, Massachusetts Institute of Technology

Abstract: Recent radio occultations of Saturn’s equatorial ionosphere by the Cassini spacecraft provide important insight into this poorly constrained region. Twelve new electron density profiles identify a clear dawn/dusk asymmetry as well as two distinct electron density peaks. This study uses a three-dimensional global circulation model along with self-consistent 1D water diffusion calculations to examine the suggestion by Connerney and Waite [1984] that a topside flux of neutral water into Saturn’s atmosphere may provide a loss mechanism - - via charge exchange with protons - - that is sufficient to reproduce the observed ionosphere. Results indicate that a constant influx of water of (0.5 – 1.0) x 107 H2O cm-2 sec-1 is adequate in reproducing

Cassini measurements, providing a good match to the main electron density peak as well as the dawn/dusk asymmetry. In addition, these calculations use a reduced rate for the controversial reaction H+ + H2(n≥4) -> H2+ + H, significantly reducing its importance in Saturn's ionospheric photochemistry. A comprehensive historical summary of outstanding issues in Saturn's ionosphere will be given to aid the unfamiliar reader.

EPAT-02 Martian Atmosphere Density Structure and Gravity Wave Variance from Mars Odyssey and MGS Accelerometer Data - by Ling Wang

Status of First Author: Non-student PhD

Authors: Ling Wang, Dave Fritts, and Robert Tolson

Abstract: Understanding the structure and dynamics of Martian atmosphere is very important to the success of any future manned or unmanned mission to Mars. Despite various unmanned Mars missions conducted during the past four decades or so, very little is known about the mean structure and dynamics of the Martian middle and upper atmosphere to this date. In this study, we use the high resolution density data from the Mars Global Surveyor (MGS) and Mars Odyssey (MO) orbiters during their respective aerobraking stages to investigate the structure and dynamics of the Martian atmosphere between ~ 100 and 160 km. Interesting spatial and temporal variations of mean densities are reported. Outstanding large scale wave structures are also found from the density data. From the very high resolution (1-second) MO data, we have the opportunity to also investigate the gravity wave variance in the same altitude range. Some preliminary results on the characteristics of the small scale waves are shown and discussed.

Index